

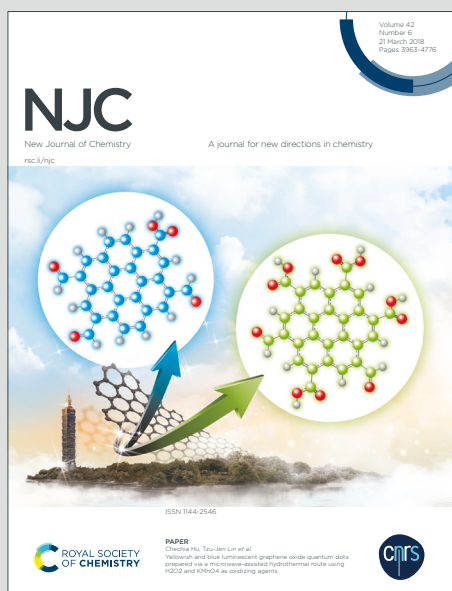
NJC

New Journal of Chemistry

Accepted Manuscript

A journal for new directions in chemistry

This article can be cited before page numbers have been issued, to do this please use: R. Bai, L. Chen, Y. Zhang, L. Chen, J. Diwu and X. Wang, *New J. Chem.*, 2020, DOI: 10.1039/D0NJ00573H.



This is an Accepted Manuscript, which has been through the Royal Society of Chemistry peer review process and has been accepted for publication.

Accepted Manuscripts are published online shortly after acceptance, before technical editing, formatting and proof reading. Using this free service, authors can make their results available to the community, in citable form, before we publish the edited article. We will replace this Accepted Manuscript with the edited and formatted Advance Article as soon as it is available.

You can find more information about Accepted Manuscripts in the [Information for Authors](#).

Please note that technical editing may introduce minor changes to the text and/or graphics, which may alter content. The journal's standard [Terms & Conditions](#) and the [Ethical guidelines](#) still apply. In no event shall the Royal Society of Chemistry be held responsible for any errors or omissions in this Accepted Manuscript or any consequences arising from the use of any information it contains.

ARTICLE

The Presence of Allovalent Silver in the Uranyl Phenylenediphosphate Framework

Ru Bai,^{a,b,§} Lanhua Chen,^{b,§} Yugang Zhang,^b Long Chen,^b Juan Diwu,^b and Xiao-Feng Wang^{*a}Received 00th January 20xx,
Accepted 00th January 20xx

DOI: 10.1039/x0xx00000x

In this work, a new 2D layered silver uranyl phosphonate compound, $\text{Ag}_{2.7}^0[\text{Ag}_8^{\text{I}}(\text{UO}_2)_6(\text{O}_3\text{PC}_6\text{H}_4\text{PO}_3)_2(\text{O}_3\text{PC}_6\text{H}_4\text{PO}_3\text{H})_4]$ (denoted as compound **1**) was synthesized by reaction of 1,2-phenylenediphosphonic acid (H_4PDPA) with $\text{UO}_2(\text{NO}_3)_2 \cdot 6\text{H}_2\text{O}$ and AgNO_3 under the mild hydrothermal condition. The uranyl layered framework consists of two types of UO_6 and UO_7 coordination units simultaneously connected by two kinds of phenylenediphosphate linkers. To our surprise, the presence of both silver ions and metallic silver atoms in the free space between the layers is identified by the single crystal X-ray diffraction, EDS, and XPS techniques. The ratio of Ag^+ and Ag^0 was estimated to be 2.81:1, based on the primary peak area of $\text{Ag } 3d_{5/2}$ from the XPS results, which corroborates with the ratio of 2.96:1 obtained from the XRD results. More importantly, the incorporation of the allovalent silver sites results in the quenching of the fluorescent emission of the uranyl phosphonate compound as evidenced by its single crystal fluorescence spectrum.

Introduction

Actinide phosphonate framework materials have attracted widespread attention in the past few decades, not only due to their adjustable structures and superior properties, but also because that phosphonates play the important role to separate uranium and plutonium in the PUREX process for the recycling of spent nuclear fuel.¹⁻⁵ Uranium is the most abundant and prior actinide element, which adopts diverse oxidation states and coordination topologies and geometries. The uranium ion is predominantly present in the hexavalent state by strongly binding with two oxo donors to form the linear triatomic uranyl unit, UO_2^{2+} . As a result, with both vertical coordination positions occupied by terminal -yl oxo groups, the uranyl unit further will be coordinated with four to six O-donor atoms from the organic ligands in the equatorial

plane, yielding UO_6 tetragonal, UO_7 pentagonal, and UO_8 hexagonal bipyramidal geometries, respectively.⁶⁻¹⁰

The phosphoric ligands can be easily prepared and readily complexed with actinides; therefore, actinide phosphonates have gradually developed into an important class of inorganic-organic hybrids. For instance, uranium phosphonates exhibit high thermal stability that originates from the extremely high binding affinity of the -CPO₃ moieties, and high structural flexibility by virtue of the various selection of the organic compartments. In addition, superior properties of uranyl phosphonate hybrid materials have been demonstrated in fields of proton conducting materials,¹¹ ion exchangers,¹² magnetism materials,¹³ and chiral materials.¹⁴ Up to date, various structure types have been reported in uranyl phosphonates including 1D chain¹⁵ and tubular, 2D layer,^{16,17} 3D framework,^{2,18} as a consequence of the uranyl hydrolysis and the uranyl complexation with phosphonic ligands through the -CPO₃ in basis η^2 and/or η^3 coordination modes.¹⁷ Multiple-topic phosphonate ligands containing more than one -CPO₃ groups and various derivatives have been designed and their uranyl coordination chemistry has been investigated to remarkably enrich the structures and topologies of uranyl phosphonates. For example, by modifying the organic skeleton,¹⁹⁻²¹ phenylphosphonate ligands were utilized to construct different low-dimensional functional architectures.

^a School of Chemistry and Chemical Engineering, and Hunan Key Laboratory for the Design and Application of Actinide Complexes, University of South China, Hengyang, 421001, China. E-mail: xfwang518@sina.cn

^b State Key Laboratory of Radiation Medicine and Protection, School for Radiological and Interdisciplinary Sciences (RAD-X), Collaborative Innovation Center of Radiation Medicine of Jiangsu Higher Education Institutions and School of Radiation Medicine and Protection, Soochow University, Suzhou 215123, China.

[§]These authors contributed equally.

Electronic Supplementary Information (ESI) available: X-ray crystallography, PXRD and TGA curve, EDS analysis, XPS and fitting parameters. CCDC 1978046. For ESI and crystallographic data in CIF or other electronic format see DOI: 10.1039/x0xx00000x

ARTICLE

Journal Name

Correspondingly, in contrast to the alkyl-phosphonic ligands, the aryl-phosphonic ligands are capable of creating a hydrophobic surface of the uranyl phosphonate hybrid materials.

Furthermore, the incorporation of alkali and/or alkali earth ions also plays an important role as structural directing agents and charge-balancing counterions. In order to increase the complexity of the architecture of actinide phosphonates, the introduction of heterometal ions as counterions and connecting nodes has attracted considerable attention. Amongst, the f-d hetero-systems supported by 3d or 4d transition metal ions (such as Co^{2+} , Zn^{2+} , Mn^{2+} , Ag^+) have been usually developed, with the emphasis on promoting the crystallization of uranyl complexes and on generating electron transitions.²²⁻²⁵ Generally, the overlap between the emission and absorption region of the f-d hybrid compounds may lead to partial quenching of its luminescent emission. But the special photoluminescent properties of the corresponding uranyl complexes by the introduction of transition metal ions and the internal and intrinsic mechanism have not been well studied.²⁶

Herein, a new bimetallic silver and uranyl phenylenediphosphonate layered coordination compound, $\text{Ag}^{0}_{2.7}[\text{Ag}^I_8(\text{UO}_2)_6(\text{O}_3\text{PC}_6\text{H}_4\text{PO}_3)_2(\text{O}_3\text{PC}_6\text{H}_4\text{PO}_3\text{H})_4]$ (compound **1**), was successfully synthesized under mild hydrothermal condition. Single crystal X-ray diffraction analysis indicated the **1** contains both metallic Ag^0 atoms and Ag^+ cations simultaneously, which were confirmed by energy dispersive spectroscopy (EDS) and X-ray photoelectron spectroscopy (XPS). Its spectroscopic properties also were studied using UV-vis-NIR absorption and fluorescence spectroscopy, and fourier transform infrared spectroscopy (FT-IR).

Experimental section

Attention! Uranium is a radioactive and chemically toxic element, and uranium-containing samples must be properly treated and protected.

All chemical reagents were purchased commercially and used without further purification. AgNO_3 and 1, 2-bis(dimethoxyphosphoryl)benzene are purchased from

Shanghai Lingfeng chemical reagent Co. Ltd and Alfa Aesar, respectively.
View Article Online
DOI: 10.1039/D0NJ00573H

Single crystal X-ray diffraction was carried out on a Bruker D8-Venture diffractometer with a Turbo X-ray Source (Mo- $\text{K}\alpha$ radiation, $\lambda = 0.71073 \text{ \AA}$) at room temperature. PXRD patterns were recorded on a Bruker D8 Advance diffractometer for Cu $\text{K}\alpha$ radiation ($\lambda = 1.54056 \text{ \AA}$) in the 2θ range of 5° to 50° . FT-IR spectra were obtained between 4000 and 400 cm^{-1} on a Thermo Nicolet iS50 spectrometer. The thermogravimetric analysis (TGA) was performed on a NETZSCH STA 449F3 instrument under a nitrogen flow. The single crystal solid-state photoluminescence and UV-vis-NIR absorption spectra were collected from a Craic Technology microspectrophotometer. X-ray photoelectron spectroscopy (XPS) was adopted on a Thermo Scientific ESCALAB 250 Xi spectrometer equipped with a monochromatic Al- $\text{K}\alpha$ X-ray source. The photoluminescence spectra of compound **1** were collected with 365 nm excitation light at room temperature.

Preparation of 1, 2-phenylenediphosphonic acid ligand (H_4PDPA): A mixture of 1,2-bis (dimethoxyphosphoryl) benzene (2 g) and excess amount of concentrated hydrochloric acid was added into a 500 mL round-bottomed flask, heated and refluxed at $120 \text{ }^\circ\text{C}$ for 72 h. Then the mixture was heated and evaporated to dry to yield the bright white powder, which was subsequently dried in a vacuum oven as the final product of H_4PDPA .²⁷

Synthesis of compound 1: The mixture of H_4PDPA (142.8 mg, 0.6 mmol), $\text{UO}_2(\text{NO}_3)_2 \cdot 6\text{H}_2\text{O}$ (150.0 mg, 0.3 mmol), AgNO_3 (138.0 mg, 0.8 mmol), and ultra-pure water (2.0 mL) were mixed in a 20 mL teflon-lined stainless steel autoclave, heated to $220 \text{ }^\circ\text{C}$ for 3 days, and then cooled down to $30 \text{ }^\circ\text{C}$ at a rate of $15 \text{ }^\circ\text{C/h}$. The products were washed with deionized water and ethanol, and then dried at $60 \text{ }^\circ\text{C}$ in a vacuum oven. The resulting blue crystalline solids compound **1** was obtained as the pure phase which was confirmed by the PXRD of bulk products according with the simulated one.

Results and discussion

Structure Description

Compound **1** crystallizes in the triclinic space group $P\bar{1}$ (Table S1), and the asymmetric unit contains three independent UO_2^{2+} units, one full-deprotonated PDPA⁴⁻ and two half-deprotonated HPDPA³⁻ ligands, 5.35 $\text{Ag}^0/\text{Ag}^{\text{I}}$ sites. As depicted in Figure 1, both U1 and U2 are chelated by four oxygens from two PDPA⁴⁻, and monodentated by one oxygen donor from the monoprotonated $-\text{O}_3$ moiety of the other HPDPA³⁻. The U1 is a pentagonal bipyramidal coordination polyhedron with the uranyl $\text{U}=\text{O}$ bond distances of 1.758(4) and 1.775(4) Å, respectively. The equatorial $\text{U}-\text{O}$ bond distances range from 2.334(4) to 2.417(4) Å. The U2 adopts a similar pentagonal bipyramidal coordination geometry as U1, where the $\text{U}2=\text{O}$ and $\text{U}2-\text{O}$ bond lengths are in the range of 1.757(5) – 1.788(5) Å and 2.196(14) – 2.418(4) Å, respectively. The BVS values of U1 and U2 are calculated to be 6.08 and 6.08 *v.u.*, respectively (see Table S2).^{28,29}

The U3 is surrounded six O atoms to form tetragonal bipyramid coordination environment which contains four monodentate oxygens in equatorial plane from four $-\text{PO}_3$ segments. Two $\text{U}=\text{O}$ bond lengths are 1.770(5) and 1.800(5) Å, while the four equatorial $\text{U}-\text{O}$ bond distances are 2.251(5), 2.258(5), 2.260(4) and 2.27(5) Å, respectively. Additionally, the results BVS value of U3 is 6.01 *v.u.* (Table S2). As shown in Figure 2, U1 and U2 units are joined together by HPDPA³⁻ and PDPA⁴⁻ ligands to form chains along the *b*-axis, which are further linked by $\text{U}3\text{O}_6$ units into a layers on $[bc]$ plane. It is interesting to note that the phenyl rings are all arranged on one side of the uranyl phosphonate layer to form the hydrophobic region, leaving the other side to be occupied by hydrophilic terminal $-\text{yl}$ oxo groups and phosphonate groups.

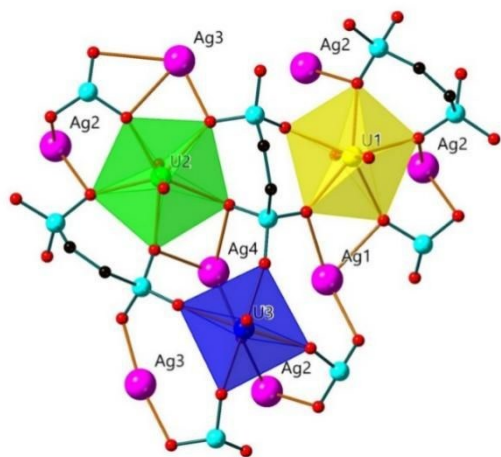


Figure 1. The representation of three uranyl coordination environments in compound **1**. (Color code: Ag, pink; C, black; P, sapphire; O, red. H atoms and part of the aromatic rings are omitted for clarity).

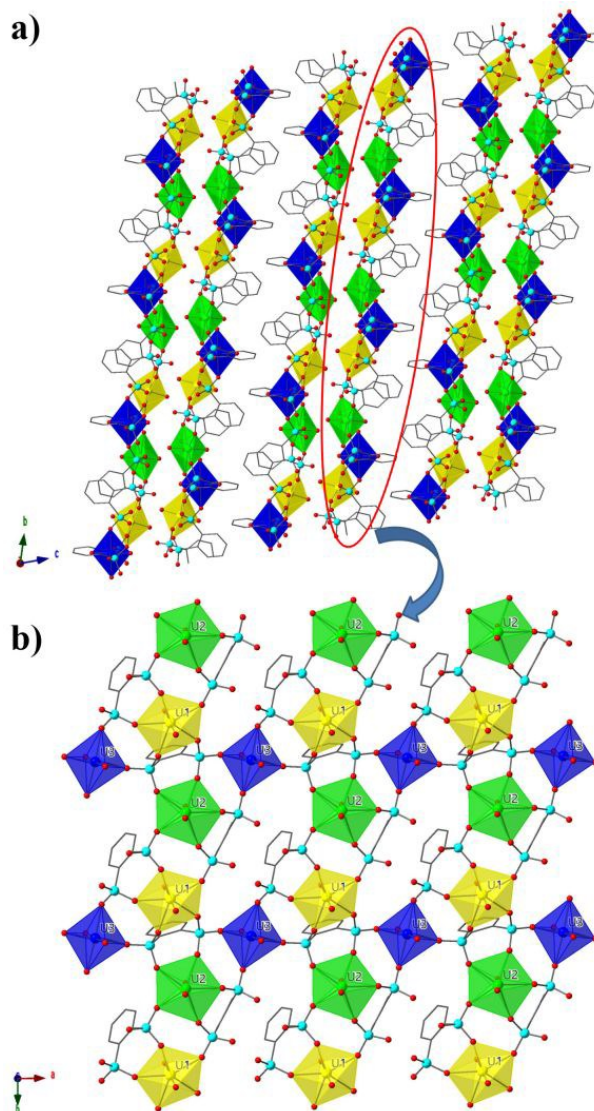


Figure 2. View of three-dimensional supramolecular structure with polyhedral uranyl of compound **1** along *a*-axis (a) and the layered expansion diagram (b). Color code: yellow polyhedron: $\text{U}(1)\text{O}_7$ unit; green polyhedron: $\text{U}(2)\text{O}_7$ unit; dark blue polyhedron: $\text{U}(3)\text{O}_6$ unit (light blue sphere: P; black sphere: C; red sphere: O. Ag^+ and Ag^0 are omitted for clarity).

The $\pi-\pi$ interaction between the phenyl rings and the hydrogen bonding interactions between the oxygen atoms result in the ABAB type stacking of adjacent layers as shown in Figure 2a.

X-ray Photoelectron Spectroscopy

X-ray Photoelectron Spectroscopy (XPS) is a widely adopted technique to investigate the chemical compositions of the

surface of materials, including the chemical valence of different elements. In **Figure S5**, the peaks of C, O, P, Ag, and U elements are all presented in the XPS survey spectra, where the binding energies (BEs) of all peaks are adjusted according to that of the C1s (284.8eV). As shown in **Figure 3**, the two strong peaks in the Ag 3d narrow-scan XPS spectrum located at 368.97 and 375 eV could be observed, which correspond to Ag 3d_{5/2} and Ag 3d_{3/2} binding energies, respectively, strongly support the presence of Ag element in compound **1**. Then, this spectrum was fitted with two Ag components of Ag⁺ and Ag⁰. As the fitting parameters are given in **Table S3**, the BEs of Ag 3d_{5/2} peaks were at 368.59 and 369.15 eV, respectively; these values are comparable with those reported in [Ag/Ag₃PO₄/GO system] (368 eV), and [CN10UA] (369.5 eV), respectively.^{30,31} Meanwhile, the calculated molar ratio of Ag⁺ to Ag⁰ is 2.81:1, based on the primary peak area of Ag 3d_{5/2}.

Taking the result of XPS into consideration, the formula of compound **1** is determined to be Ag⁰_{2.7}[Ag^I₈(UO₂)₆(O₃PC₆H₄PO₃)₂(O₃PC₆H₄PO₃H)₄], where Ag⁺ cations compensate the negative charge of the uranyl layer. In this formula, the ratio of Ag to U also corroborates with the ratio obtained from the EDS (Figure S2) and the single crystal XRD results. It is noteworthy that coordination compounds containing Ag⁰ is exceeding rare. For example, to date, only two MOF materials containing Ag⁰ have been reported, where the Ag⁰ was proposed to originate from the reduction of the Ag⁺ ion with the aid of the DMF solvent.^{32,33} In our previous work, we have also noticed the thermal reduction of U(VI) to U(IV) in solvothermal reactions without the presence of silver ions.³⁴ Therefore, we also speculate that the reduction of Ag⁺ occurred under the hydrothermal condition, affording the allovervalent silver uranyl phosphonate compound.

Spectroscopic Properties.

The UV-vis-NIR spectrum of the compound **1** was collected at room temperature, as shown in **Figure 4a**. The peak at ca. 278 nm is assigned to the axial U=O charge transfer, which is the characteristic absorption peak of the uranyl unit. The peaks ranging from 420 to 640 nm are ascribed to the ligand to metal charge transfer (LMCT) between the O atoms from ligand and empty orbitals from the uranyl units.^{35,36} The fluorescence spectra of H₄PDPA ligand, uranyl nitrate hexahydrate, and

compound **1** under UV light excitation at 365 nm are shown in **Figure 4b**.
DOI: 10.1039/D0NJ00573H

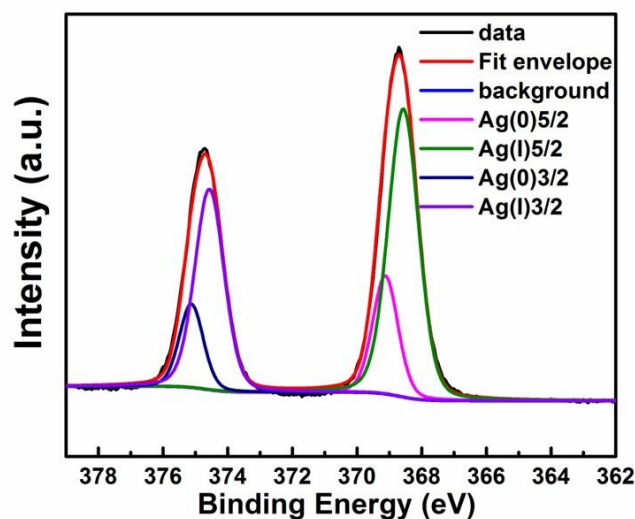


Figure 3. Ag 3d XPS spectra of compound **1**.

The spectrum of the pristine H₄PDPA ligand displays one strong and broad emission peak between 410 and 600 nm, which corresponds to the π - π^* transition of the phenyl groups. The spectrum of uranyl nitrate hexahydrate exhibits the classic fluorescence pattern of the UO₂²⁺ unit that consists of several strong emissions located at 486, 510, 530, 558, and 590 nm, respectively. The typical uranyl emission arises from the electronic and vibronic transitions S₁₀ – S_{0v} (v = 0–4) and S₁₁–S₀₀ of the symmetrical and antisymmetric modes of the uranyl centre.^{20,22,37} The emission spectra of uranyl phosphonate compounds that contain Ag⁺ have been reported to exhibit the typical uranyl emission patterns.^{38,39} In sharp contrast, the emission of the U(VI) units in compound **1** was completely quenched as shown in **Figure 3b**, probably owing to the presence of the Ag⁰.

The FT-IR spectrum of compound **1** was further collected to characterize its structural features as shown in **Figure S3**. Peaks at 900-920 cm⁻¹ are attributed to the asymmetric stretching frequency $\nu_{as}(\text{O}=\text{U}=\text{O})$, while those at the 820-840 cm⁻¹ are ascribed to the symmetric stretching frequency modes.^{19,40} The bands in the range of 1400~1565 cm⁻¹ for compound **1** are assigned to the stretch of the aromatic rings.¹⁷ The characteristic antisymmetric and symmetric stretch peaks of the P=O and P-O moieties are presented

between 990-1257 cm^{-1} , while the peaks from 750 to 775 cm^{-1} can be assigned to the P-C bonds.^{19,39} The peak located at 593 cm^{-1} is attributed to the Ag-O stretching vibrations according to the literature report.⁴¹

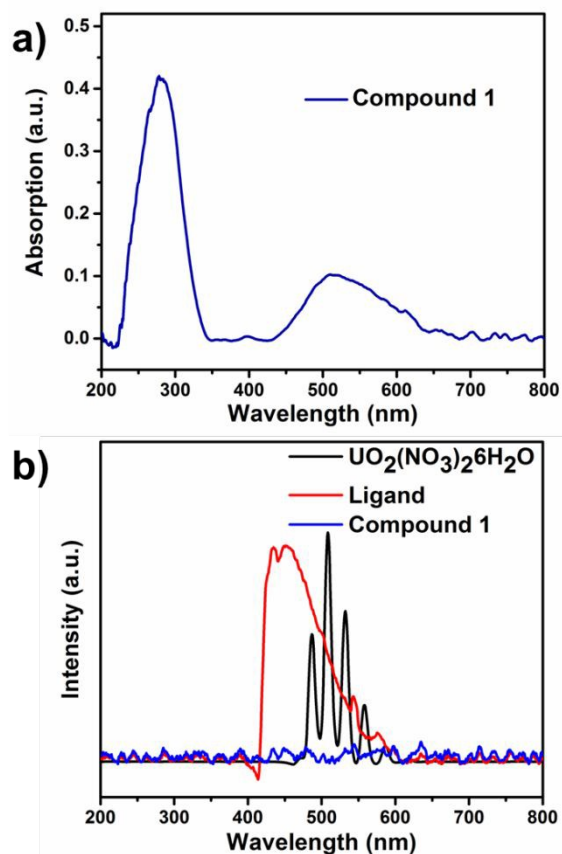


Figure 4. (a) UV-vis-NIR absorption spectrum and (b) luminescence spectra of compound 1, H_4PDPA ligand, and $\text{UO}_2(\text{NO}_3)_2 \cdot 6\text{H}_2\text{O}$.

Conclusion

In this work, a stable silver uranyl phenylenediphosphonate coordination compound is synthesized, and structurally and spectroscopically characterized. It is worth noting that our results demonstrate the unique presence of the alvalent silver in the uranyl phosphonate layered framework. Specifically, it is the existence of Ag^0 rather uranyl emission that was observed in the luminescence spectrum. It is believed that this result could shed some light on the design and synthesis of novel alvalent silver uranyl coordination compound.

Conflicts of interest

There are no conflicts to declare.

Acknowledgements

This work is supported by the National Natural Science Foundation of China (No.11375082, 51802147, 21906113 and 21806117) and a project funded by Jiangsu Provincial Key Laboratory of Radiation Medicine and Protection.

Notes and references

- W.-T. Yang, T. G. Parker, Z.-M. Sun, *Coord. Chem. Rev.*, 2015, **303**, 86-109.
- P. O. Adelani, A. G. Oliver, T. E. Albrecht-Schmitt, *Cryst. Growth Des.*, 2011, **11**, 3072-3080.
- A. G. D. Nelson, T. H. Bray, F. A. Stanley, T. E. Albrecht-Schmitt, *Inorg. Chem.*, 2009, **48**, 4530-4535.
- T. G. Parker, J. N. Cross, M. J. Polinski, J. Lin, T. E. Albrecht-Schmitt, *Cryst. Growth Des.*, 2014, **14**, 228-235.
- A. G. D. Nelson, T. H. Bray, W. Zhan, R. G. Haire, T. S. Sayler, T. E. Albrecht-Schmitt, *Inorg. Chem.*, 2008, **47**, 4945-4951.
- Y. -L. Wang, Z. -Y. Liu, Y. -X. Li, Z. -L. Bai, W. Liu, Y. -X. Wang, X. -M. Xu, C. -L. Xiao, D. -P. Sheng, J. Diwu, J. Su, Z. -F. Chai, T. E. Albrecht-Schmitt, S. -A. Wang, *J. Am. Chem. Soc.*, 2015, **137**, 6144-6147.
- P. Li, N. A. Vermeulen, C. D. Malliakas, D. A. Gómez-Gualdrón, A. J. Howarth, B. L. Mehdi, A. Dohnalkova, N. D. Browning, M. O'Keeffe, O. K. Farha, *Science*, 2017, **356**, 624-627.
- M. B. Andrews, C. L. Cahill, *Chem. Rev.*, 2013, **113**, 1121-1136.
- V. Smetana, S. P. Kelley, H. M. Titi, X. -M. Hou, S. -F. Tang, A. -V. Mudring, R. D. Rogers, *Inorg. Chem.* 2020, **59**, 818-828.
- X. -M. Hou, S. -F. Tang, *RSC Adv.*, 2014, **4**, 34716-34720.
- D.-X. Gui, W.-C. Duan, J. Shu, F.-W. Zhai, N. Wang, X.-X. Wang, J. Xie, H. Li, L.-H. Chen, J. Diwu, Z.-F. Chai, S.-A. Wang, *CCS Chem.*, 2019, **1**, 197-206.
- P. O. Adelani, T. E. Albrecht-Schmitt, *Angew. Chem. Int. Ed.*, 2010, **49**, 8909-8911.
- L.-H. Chen, T. Zheng, S.-S. Bao, L.-J. Zhang, H.-K. Liu, L. -M. Zheng, J.-Q. Wang, Y. -X. Wang, J. Diwu, Z. -F. Chai, T. E. Albrecht-Schmitt, S. -A. Wang, *ChemPubSoc Europe.*, 2016, **22**, 11954-11957.
- J. Diwu, T. E. Albrecht-Schmitt, *Chem. Comm.*, 2012, **48**, 3827-3829.
- D. Grohol, F. Gingl, A. Clearfield, *Inorg. Chem.*, 1999, **38**, 751-756.
- H. -Y. Wu, W. -T. Yang, Z.-M. Sun, *Cryst. Growth Des.*, 2012, **12**, 4669-4675.
- W. -T. Yang, T. Tian, H.-Y. Wu, Q. -J. Pan, S. Dang, Z.-M. Sun, *Inorg. Chem.*, 2013, **52**, 2736-2743.
- W.-T. Yang, H.-Y. Wu, R. -X. Wang, Q. -J. Pan, Z. -M. Sun, H. -J. Zhang, *Inorg. Chem.*, 2012, **51**, 11458-11465.
- C. Liu, W. T. Yang, N. Qu, L. -J. Li, Q.-J. Pan, Z. -M. Sun, *Inorg. Chem.*, 2017, **56**, 1669-1678.

ARTICLE

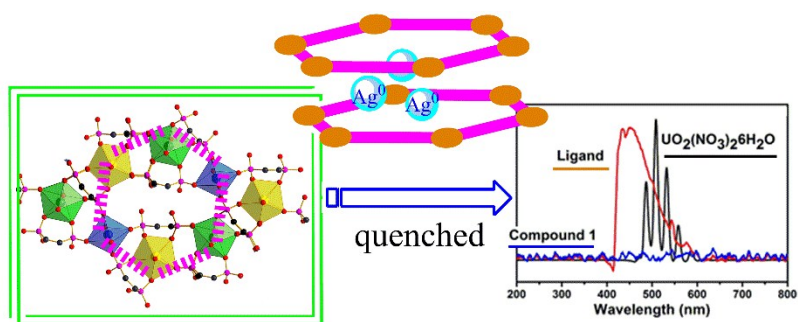
Journal Name

- 20 S.-F. Tang, X. -M. Hou, D.-D. Liu, X.-B. Zhao, *Inorg. Chem.*, 2017, **56**, 14524-14532.
- 21 B. Monteiro, J. A. Fernandes, C. C. L. Pereira, S. M. F. Vilela, J. P. C. Tomé, J. Marcalo, F. A. A. Paz, *Acta Cryst.*, 2014, **B70**, 28–36.
- 22 X. -M. Hou, S. -F. Tang, *Inorg. Chim. Acta.*, 2018, **474**, 11-15.
- 23 X. -M. Hou, S. -F. Tang, *RSC Adv.*, 2016, **6**, 100158–100166.
- 24 S.-F. Tang, X. -M. Hou, *Inorg Chem.*, 2019, **58**, 1382-1390.
- 25 A. N. Alsobrook, W. Zhan, T. E. Albrecht-Schmitt, *Inorg. Chem.* 2008, **47**, 5177-5183.
- 26 P. O. Adelani, T. E. Albrecht-Schmitt, *Inorg Chem.*, 2010, **49**, 5701-5705.
- 27 J. Diwu, S. -A. Wang, Z. -L. Liao, P. C. Burns, T. E. Albrecht-Schmitt, *Inorg. Chem.* 2010, **49**, 10074–10080.
- 28 P. C. Burns, *Can. Minera.*, 2005, **43**, 1839-1894.
- 29 B. N. E. Brese, M. O'Keeffe, *Acta. Cryst.*, 1991, **B47**, 192-197.
- 30 T. Kusutaki, H. Katsumata, I. Tateishi, M. Furukawa, S. Kaneco, *RSC Adv.*, 2019, **9**, 39843-39853.
- 31 M. -S. Zhu, P. -L. Chen, M. -H. Liu, *Chin. Sci. Bull.*, 2013, **58**, 84-91.
- 32 H.-X. Guo, Y. -H. Zhang, Z. -S. Zheng, H. -B. Lin, Y. Zhang, *Talanta*, 2017, **170**, 146-151.
- 33 W. S. Abo El-Yazeed, A. I. Ahmed, *RSC Adv.*, 2019, **9**, 18803-18813.
- 34 L. -H. Chen, J. Diwu, D. -X. Gui, Y. -X. Wang, Z. -H. Weng, Z. -F. Chai, T. E. Albrecht-Schmitt, S. -A. Wang, *Inorg. Chem.*, 2017, **56**, 6952-6964.
- 35 X. Zhao, D. Zhang, Y. Ren, S. -S. Chen, D. -H. Zhao, *Eur. J. Inorg. Chem.*, 2018, **10**, 1185-1191.
- 36 H. -H. Li, X. -H. Zeng, H. -Y. Wu, X. Jie, S. -T. Zheng, Z. -R. Chen, *Cryst. Growth Des.*, 2015, **15**, 10-13.
- 37 R. Zhao, L. Mei, K. -Q. Hu, M. Tian, Z. -F. Chai, W. -Q. Shi, *Inorg Chem.*, 2018, **57**, 6084-6094.
- 38 A. G. D. Nelson, Z. Rak, T. E. Albrecht-Schmitt, R. C. Ewing, *Inorg. Chem.*, 2014, **53**, 2787-2796.
- 39 P. O. Adelani, T. E. Albrecht-Schmitt, *Cryst. Growth Des.*, 2012, **12**, 5800-5805.
- 40 R. A. Cozaciuc, R. Postolachi, R. Gradinaru A. Pui, *J. Coord. Chem.*, 2012, **65**, 2170-2181.
- 41 M. A. Girsovaa, G. F. Golovinaa, I. N. Anfimovaa, L. N. Kurilenko, *Glass. Phys. Chem.*, 2019, **45**, 325-331.

View Article Online
DOI: 10.1039/D0NJ00573H

New Journal of Chemistry Accepted Manuscript

TOC



A 2-D silver uranyl phosphonate present both Ag^+ and Ag^0 atoms in the free space between the adjacent layers and the incorporation of the aliovalent silver sites results in the quenching of the fluorescent emission.